Front. Earth Sci. 2024, 18(2): 446–459
https://doi.org/10.1007/s11707-022-1073-3

RESEARCH ARTICLE

# Astronomical forcing and sedimentary noise modeling of lake-level changes in the Middle Eocene Chezhen Sag, Bohai Bay Basin, eastern China

**Xuwei LUAN[1], Jinliang ZHANG (✉)[1], Na LI[1], Tao CHEN[1], Long SUN[2], Xuecai ZHANG[3]**

1 Faculty of Geographical Science, Beijing Normal University, Beijing 100875, China
2 College of Geosciences, China University of Petroleum (Beijing), Beijing 102249, China
3 Management Center of Oil and Gas Exploration, Sinopec Shengli Oilfield, Dongying 257000, China



**Abstract** The accurate determination of geological age is a key to understanding the history and process of paleolake evolution and oil and gas exploration in continental lake basin. However, improving the accuracy of geological age has always been a difficult scientific problem. A 609-m-thick, continuous lacustrine mudstone and sandstone succession in Chezhen Sag (eastern China) provides an ideal middle Eocene sedimentary record for establishing a high-resolution stratigraphic chronology framework. Based on spectrum analysis and sliding window spectrum analysis of the natural gamma (GR) logging data of well Che 271 (C271) in Chezhen Sag, the periods of 405 kyr and 40.1 kyr were filtered by a Gaussian bandpass filter, and a "floating" astrochronological time scale (ATS) was established. The total number of 405 kyr eccentricity cycles were 13.6 and 40.1 kyr obliquity cycles were 138 which recorded from the upper member 4 (Es4U) to the member 3 (Es3) of the Eocene Shahejie Formation, and the depositional duration was 5.53 Myr. Correlation Coefficient (COCO) analysis and evolutionary Correlation Coefficient (eCoCo) analysis found that the optimal sedimentary rate of different strata. Sedimentary noise simulation revealed the history of paleolake water changes in the Middle Eocene in the Chezhen Sag, according to which four sequences are divided. The study shows that the lake level change of Chezhen Sag in the middle Eocene shows prominent 1.2 Myr cycles and an antiphase well-coupled relationship with obliquity modulation. Finally, we propose a model to explain the relationship between the orbital cycle and lake level change in the continental lake basin. When the obliquity of the earth increases, the middle and high latitudes of the earth will be closer to the sun, the direct sunlight will be higher, and the meridional sunshine will increase, thus accelerating the evaporation process of lake basin water. When the seasonal changes are obvious (maximum period of 1.2 Myr ultra-long obliquity), this effect is more significant. The relative lake level change based on the restoration of high-precision ATS has significant scientific and economic value for understanding the vertical evolution of continental stratigraphic sequences and the formation and distribution of oil and gas resources.

**Keywords** Chezhen Sag, cyclostratigraphy, astrochronological time scale, sedimentary noise

## 1 Introduction

The Bohai Bay Basin is China's most productive petroliferous basin, accounting for approximately one-third of China's total oil production (Hao et al., 2009). High-quality source rocks have been widely developed in the Paleogene and Middle Eocene, mainly lacustrine fine-grained sedimentary rocks with continuous deposition and large thickness (Hao et al., 2009; Feng et al., 2016). Lacustrine fine-grained sedimentary rock particles have particles smaller than 62.5 μm, and their main components include clay minerals, silt, carbonate, and organic matter (Freytet and Verrecchia, 2002; Aplin and Macquaker, 2011). Because of their uninterrupted nature and high resolution, they can be used as a good recorder of paleoclimate information (Luan et al., 2022). However, accurately extracting Milankovich cycle signals from lacustrine sedimentary records and eliminating the interference of unexpected events or nonastronomical periodic signals are complex problems.

In the early 1840s, Milankovich put forward the hypothesis that under the influence of other celestial bodies, the orbital parameters of the earth will change

Received October 26, 2022; accepted April 10, 2023

E-mail: jinliang@bnu.edu.cn

periodically in the process of rotation and revolution, thus driving the variation in solar radiation at different latitudes and seasons (Hinnov, 2013). Hays et al. (1976) studied deep-sea sediments in the Southern Hemisphere that accumulated over 450000 years. Using the oxygen isotope ($\delta^{18}O$) in the deposits as a substitute index, the closely related climate change signals were obtained by spectral analysis, which revealed that the periodic variation in the Earth's orbit was the reason for the alternation of glacial and interglacial periods, and the Milankovich hypothesis has been verified. Subsequently, cyclostratigraphy based on Milankovich's theory has been widely recognized and widely used in the field of Earth and planetary science for nearly half a century (Hinnov and Hilgen, 2012; Hinnov, 2013; Huang, 2014). Cyclostratigraphy holds that the influence of the periodic change in Earth's orbit on the sedimentary records is due to the regulation of solar radiation, thus affecting the periodic change in Earth's climate, and these climate fluctuations are recorded in the sediments, forming a stratigraphic cycle consistent with the period of the Earth's orbital parameters (Wu et al., 2014; Huang and Hinnov, 2019). The periodic signals in these sedimentary sequences are identified and extracted by mathematical and statistical methods, concerning the theoretical astronomical cycle solution (Laskar et al., 2011). A high-resolution astronomical chronograph (ATS) was established to realize high-precision stratigraphic division and correlation (Yao et al., 2015; Li et al., 2016; Liu et al., 2018).

An extensive set of continuous lacustrine fine-grained sedimentary rocks have developed in Chezhen Sag, which is less affected by the geological structure, more sensitive to climate change, and suitable for the extraction and recognition of astronomical cycle signals. Previous researchers have made valuable progress in studying cyclic stratigraphy in the Dongying Sag and Zhanhua Sag of the Bohai Bay Basin. Liu et al. (2018) used high-resolution GR logging data and Multi-taper method (MTM) spectrum analysis, and the astronomical time scale of Paleogene strata in the Dongying Sag was established. The absolute age of the boundary between Es3 and Es4 is 42.47 Ma. Based on this, Zhang and Jin (2021) established the astronomical time scale of the lower member 3 (Es3L) strata in Zhanhua Sag. Shi et al. (2019), through the study of comprehensive magnetostratigraphy, determined the boundary between C18n1n/C18n1r and C19n/C19r in GTS2012, which provides the possibility for the recalculation of stratigraphic age in the Jiyang Depression. However, previous work on cyclic stratigraphy in Chezhen Sag is insufficient. The research on the evolution of the paleoenvironment in the target section of the study area is inadequate and requires further examination.

In previous studies, eccentricity is considered to be closely related to monsoon and precipitation (Jin et al., 2020). In recent years, scholars have found that the 1.2 Myr ultra-long obliquity is one of the main driving forces for the rise and fall of sea/lake levels. A 1.2 Myr ultra-long obliquity period comes from the change of inclination angles of Mars and Earth orbits (s4-s3) (Laskar et al., 2004; Hinnov and Hilgen, 2012; Huang, 2014), and is recorded in many strata. Wang et al. (2020) reconstructed lake level changes in the Paleoproterozoic strata of the Dongpu and Qianjiang Sags by sedimentary noise model analysis and found that the high-resolution lake level change curves reconstructed from tuned gamma-ray sequences are related to the million-year-scale (e.g., 2.4 Myr and 1.2 Myr) astronomical drivers, revealing a link between lake level evolution in terrestrial basins and long-term astronomical drivers. Zhang et al. (2022) used the GR and Th sequences of three wells in Songliao Basin in the Late Cretaceous as surrogate indexes for cycle analysis, and the ancient lake level change in Songliao Basin recovered from the sedimentary noise model showed a remarkable 1.2 Myr cycle, which was well coupled with the obliquity amplitude modulation.

In this study, the strata from Es4U to Es3 of C271 in Chezhen Sag are the research object, and the stable and reliable Milankovich cycle signal was identified using the cycle analysis method. The Middle Eocene "floating" astronomical time scale in Chezhen Sag is established, which provides new ideas and guidance for the exploration and development of continental shale oil in China under the constraint of an acceptable chronostratigraphic framework and paleodepositional environment evolution analysis.

## 2 Geological setting

The Bohai Bay Basin is a Cenozoic rift basin formed in the basement of the North China Craton, with an area of approximately 200000 km$^2$ (Li et al., 2014). The Jiyang Depression is the most oil-gas-rich area in the Bohai Bay Basin and is divided into four sags. The Chezhen Sag, located on the northern margin of the Jiyang Depression, covers an area of 2390 km$^2$. It is an "S"-type continental dustpan-like fault basin with north faulting and south surpassing and near the east–west strike, which is the focus of this study (Fig. 1(a)). A series of faults further divide it into four sub-sags, which are the Chexi Sub-Sag, Taoerhe Sub-Sag, Dawangbei Sub-Sag, and Guojuzi Sub-Sag from west to the east (Fig. 1(b)) (Su et al., 2011). All sub-sags are interconnected through the saddle between nose structures and have similar evolutionary characteristics (Wang and Cao, 2010). The borehole used in this study is located in the Chexi Sub-Sag (C271) (Fig. 1(b))

The Kongdian Formation, Shahejie Formation, and Dongying Formation developed from bottom to top in the Paleogene of the Chezhen Sag. The Shahejie Formation is divided into the fourth (Es4), third (Es3), second (Es2),

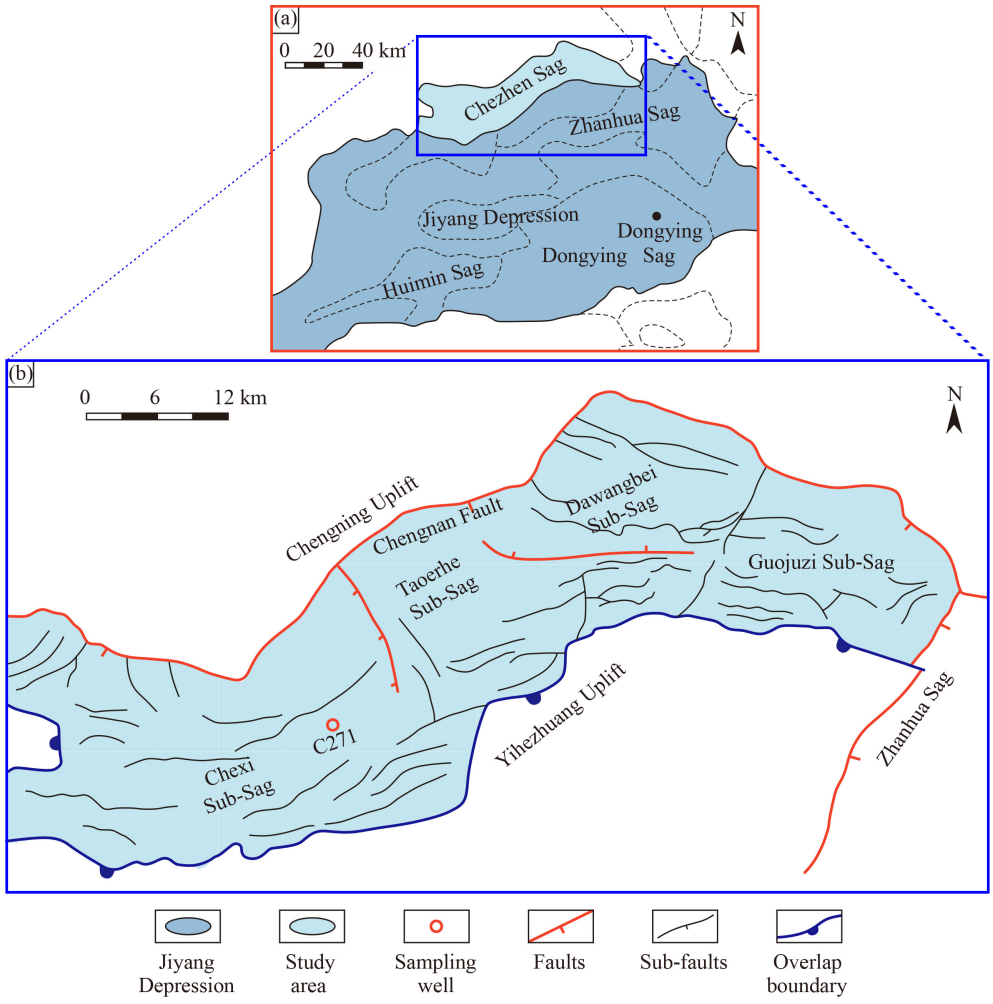


**Fig. 1** Geological setting of the Chezhen Sag, eastern China. (a) Location of the Chezhen Sag in the Bohai Bay Basin; (b) Structural features and sampling well location of the Chezhen Sag.

and first (Es1) members of the Shahejie Formation from bottom to top (Fig. 2). The fourth and third members of the Paleogene Shahejie Formation are a set of lacustrine deposits dominated by mudstone and sandstone. They are the main oil-generating layers and reservoirs in the study area, and they are also the study intervals at this time. During this period, the Chezhen Sag was in the development period of the extensional fault sag (stage II and stage III (Fig. 2)) (Chen et al., 2021). The structure of the fault sag was relatively straightforward, which was steep in the north and gentle in the south (Figs. 2(b) and 2(c)) (Wang, 2017). C271 is located in the Chexi Sub Sag. Throughout the Es4 to Es3 period, there was no sedimentary discontinuity, and a large set of fine-grained sediments developed, which is suitable for identifying and extracting astronomical cycles.

The existing chronostratigraphic framework in the Bohai Bay Basin is based on a combination of radioactive and paleomagnetic dating (Liu et al., 2018). A study by Yao et al. (1994) showed that the absolute isotopic age of volcanic rocks in Es3 and Es4 in the oil and gas area of the Bohai Bay Basin is 42.4 Ma (Fig. 2(i)). Shi et al. (2019) studied comprehensive magnetostratigraphy, and the boundary between C18n1n/C18n1r and C19n/C19r was determined in GTS2012, which provides the possibility for the recalculation of stratigraphic age in the Jiyang Depression. However volcanic ash dating is limited by acquiring suitable dating materials and the scope of age application. It correlates poorly with distant sedimentary sequences (deep sea, lakes, etc.) (Chen et al., 2014). Due to the technical limitations at that time, there were some problems with the accuracy of the results measured by Yao et al. (1994) Therefore, in this paper, the anchor point of the “floating” astronomical time scale in the Chezhen Sag will use the C19n bottom age 41.39 Ma measured by Shi et al. (2019) which corresponds to the demarcation point of Es3 and Es4 (Fig. 2(j)).

## 3 Materials and methods

### 3.1 GR logging data

The GR logging curves correspond well with the contents

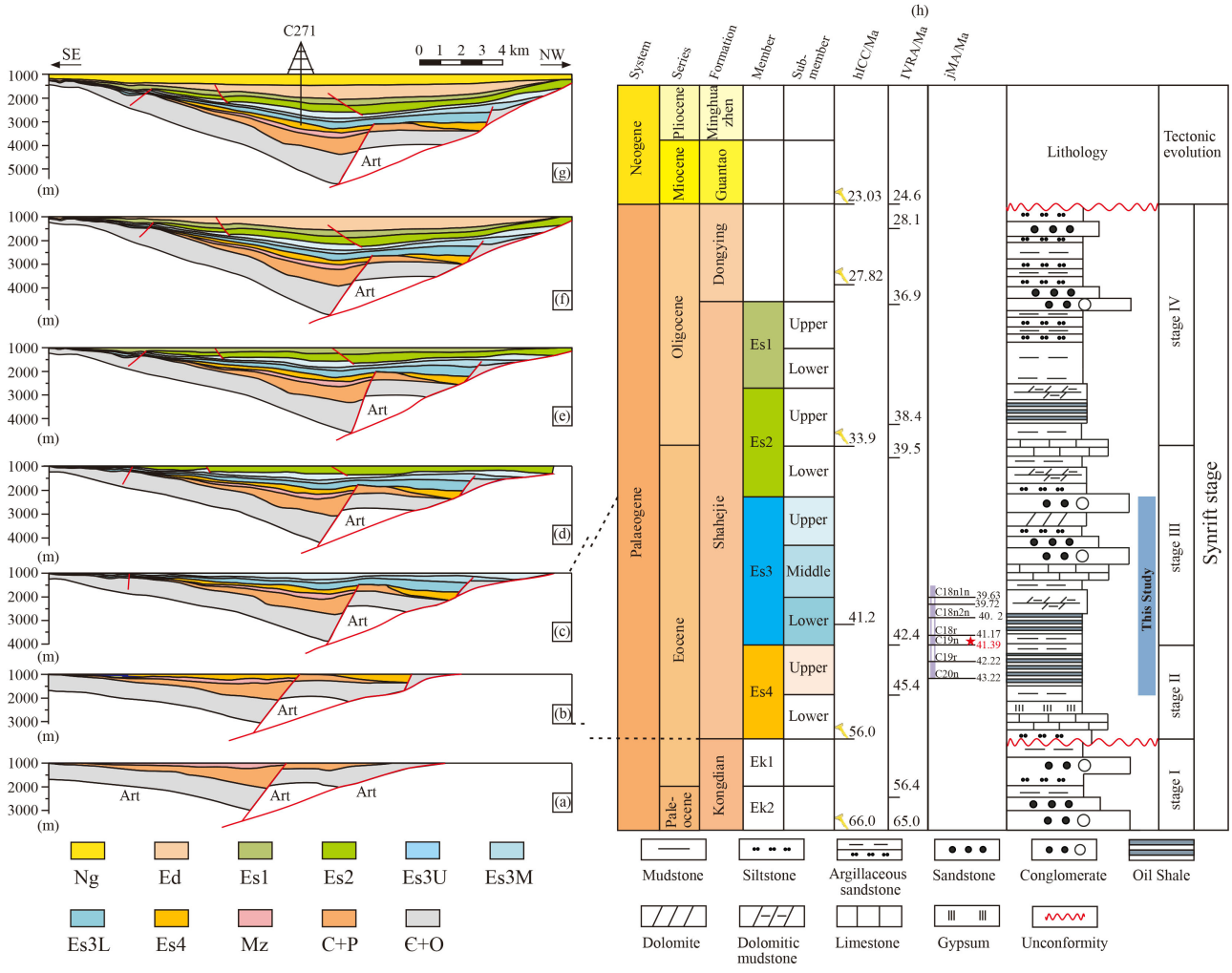


**Fig. 2** The Paleogene age framework of the Chezhen Sag. (a–g) The history of tectonic evolution in the north–south direction of the Chexi Sub-Sag. (h) ICC, International Chronostratigraphic Chart, 2022. (i) Volcanic Rock Age (VRA) in Bohai Bay Basin (Yao et al., 1994). (j) Magnetic Age (MA) in Jiyang Depression (Shi et al., 2019).

of clay and organic matter, which are related to the fluctuation of the sea or lake water level and the input of terrigenous debris caused by climate change. High GR values indicate high levels of clay and organic matter, corresponding to warm climates (van Vugt et al., 2001; Wu et al., 2014; Liu et al., 2018). Therefore, the GR logging curves can be used as a paleoclimate indicator to establish an astronomical time scale.

In this study, the GR logging data of C271 were collected by the Shengli Oilfield Logging Company, and all rock samples were analyzed and tested by the Shengli Oilfield Exploration and Development Research Institute. We selected the GR data set of Es4U-Es3 in the lower part of C271 (2291−2900 m, the top of Es3 was 2291 m; the bottom of Es4U was 2900 m, and the thickness was 609 m). Es3 can be divided into Es3L (2465−2677.5 m, the thickness was 212.5 m), the middle member 3 (Es3M) (2385−2465 m, the thickness was 80 m), and the upper member 3 (Es3U) (2291−2385 m, the thickness was 212.5 m) from bottom to top. Es4 was not completely drilled, and Es4 in the conditioned part is Es4U (2677.5−2900 m, the thickness is 222.5 m).

### 3.2 Time series methods

Continental strata have the characteristics of substantial heterogeneity and unstable sedimentary rates, so it is essential to eliminate the interference signals caused by geological tectonic activities or erratic events to identify the actual Milankovich cycle signal. Data preprocessing methods such as past extreme values and detrending are often used to remove noise signals from geological records. Through segmented spectrum analysis, the sedimentation rate is matched to improve the accuracy of Milankovich cycle signal recognition. The specific processing methods are as follows.

1) Remove the extremes and the singularities of a data set.

2) Interpolation. The GR logging sequence was linearly interpolated to obtain an evenly spaced data set with a sampling rate of 0.125 m.

3) Remove the trend. While reducing the trend interference, it is also necessary to avoid the distortion of the low-frequency signal of the spectrum, and a 20% weighted average operation is carried out on the GR logging data.

4) Spectral analysis of the GR log series was performed using the 2Π MTM method (Thomson, 1982). In addition, Fast Fourier transform (FFT) spectra were obtained on the GR logging sequence to track the change in cycle frequency under different sedimentary rates. The relationship between the deposition cycles and earth orbit parameters was determined by the cycle length ratio method.

5) The COCO and eCOCO analysis were applied to the detrended GR sequence to provide strong evidence for cyclic stratigraphic interpretation and obtain the final sedimentary rate.

6) Finally, the tilt period of 405 kyr is extracted by a Gaussian bandpass filter, and then the astronomical time scale is established as a metronome.

7) The theoretical astronomical model La2010d (Laskar et al., 2011) was compared with the astronomically tuned composite GR record.

The above data processing and calculation methods are based on AcycleV2.4 software under the MATLAB platform (Li et al., 2019).

### 3.3 Sedimentary noise modeling

The sedimentary noise model, developed by Li et al. (2018), is a method which can reconstruct changes in ancient sea and lake levels by analyzing the sedimentary noise intensity of stratigraphic sequence. This approach provides insights for studying ancient water level changes in deep time (Li et al., 2018; Wang et al., 2020). The sedimentary noise models include the Lag-1 autocorrelation coefficient method ($\rho$1) and dynamic noise after orbit tuning (DYNOT). The two methods are independent of each other, but they can verify each other. $\rho$1 is an index that can independently test the change in relative water level, and both depth series and time series can be used as objects for data analysis. DYNOT can carry out energy spectrum analysis of paleoclimate time series, measure noise in climate and water depth indices, and evaluate the energy ratio of non-astronomical signals (noise) to the total energy. This method can only be applied to time domain (tuned) data series. Generally, a high noise data set corresponds to a high DYNOT value and a low $\rho$1 value, indicating a shallow water depositional environment; a low noise data set corresponds to a low DYNOT value and a high $\rho$1 value, indicating a deep water depositional environment.

## 4 Results

### 4.1 Theoretical astronomical cycle

This study was based on the solution of La2010d (Laskar et al., 2011). The theoretical values of eccentricity, obliquity, and precession variation (E + O-P) between 35 and 45 Ma were calculated, and the sampling interval was 1 kyr (Fig. 3(a)). The obtained curve is analyzed by MTM spectrum analysis and sliding window spectrum analysis. The spectrum diagram (Fig. 3(b)) and the sliding window spectrum diagram (Fig. 3(c)) were obtained. The main astronomical periods during 35–45 Ma in Chezhen Sag are 405 kyr, 125 kyr, 96.9 kyr, 51.7 kyr, 40.1 kyr, 38.7 kyr, 23.2 kyr, 22.0 kyr, and 18.7 kyr. Among them, 405 kyr (E1), 125 kyr (E2), and 96.9 kyr (E3) belong to the eccentricity cycle; 51.7 kyr (O1), 40.1 kyr (O2), and 38.7 kyr (O3) belong to the obliquity cycle; and 23.2 kyr (P1), 22.0 kyr (P2), and 18.7 kyr (P3) belong to the precession cycle (Fig. 3(b)).

### 4.2 Depth Domain Spectrum Analysis of C271

The lithologic interface of Es4U and Es3 in C271 is located at 2677.5 m. The amplitude and frequency of the GR sequences are lower than those of Es4U (Fig. 4(a)). The untreated GR logging curve tends to decrease at first and then increase with increasing depth (Fig. 4(a)), this may be the signal produced by the long-period tectonic evolution or the cycle signal independent of the astronomical period caused by the influence of formation temperature and pressure on the logging curve in the formation (Zhou et al., 2022). Previous studies have shown that the sedimentation rate of Es4–Es3 strata in Bohai Bay Basin is approximately 0.1–0.2 m/kyr (Liu et al., 2018). The thickness of the sedimentary cycle controlled by the long eccentricity cycle (405 kyr) is approximately 40–80 m. While reducing the trend interference, it is also necessary to avoid the distortion of the low-frequency signal of the spectrum. The length of the sliding window is generally 1.5–2 times the thickness of the sedimentary cycle controlled by the long eccentricity (Li et al., 2019). Therefore, a 20% weighted average operation of GR logging data are carried out in this study.

The detrended GR logging data (Fig. 4(b)) are analyzed by 2 Π MTM spectrum analysis (Fig. 4(d)) and FFT sliding window spectrum analysis (Fig. 4(c)). The step length of the sliding window was 0.97 m, and the window length was 121.8 m. The results of spectrum analysis show that the thickness (reciprocal of frequency) corresponding to the peak in the sliding window map indicates that the signals of eccentricity, obliquity, and precession were preserved in the target formation (Fig. 4(d)). However, the frequency corresponding to the

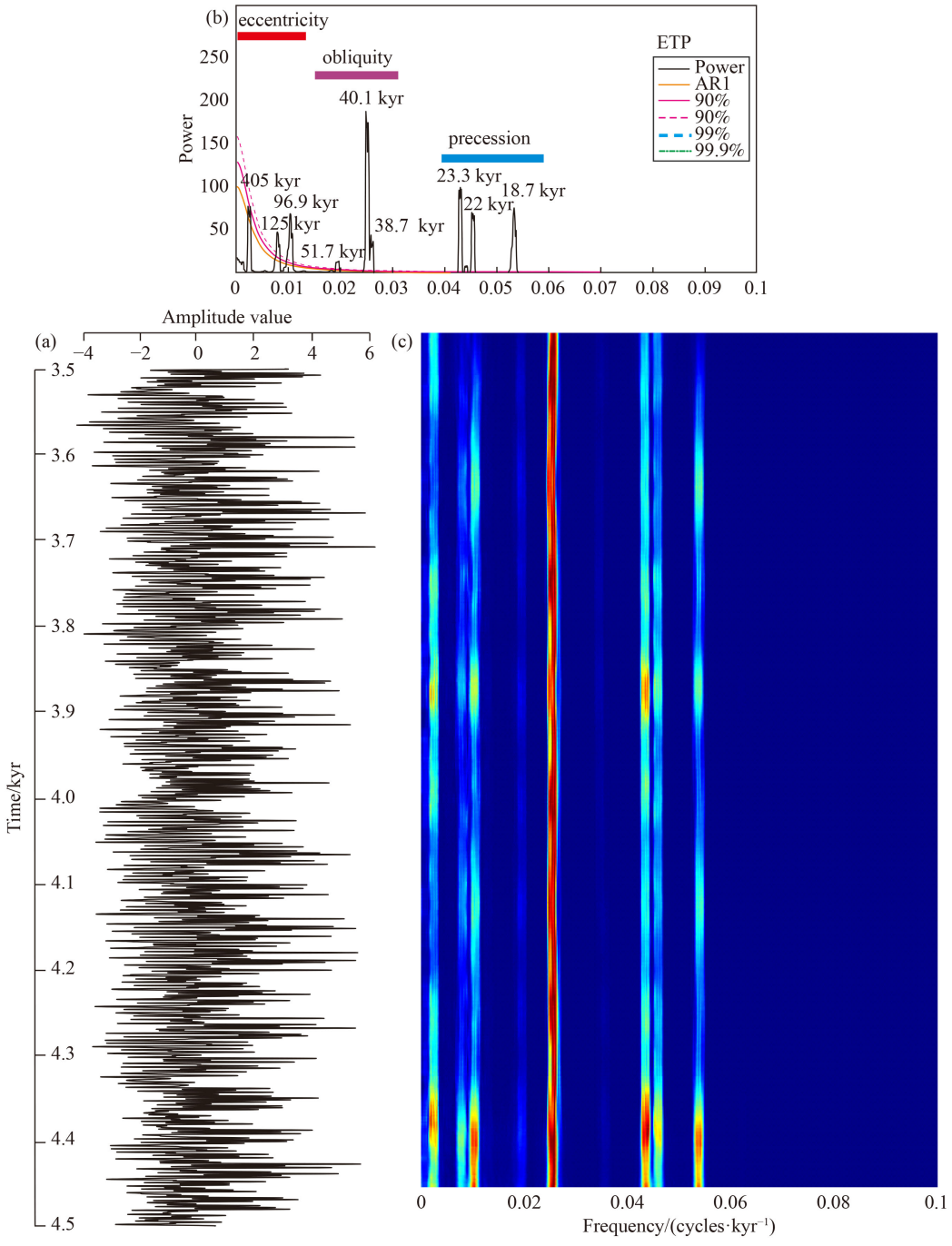


**Fig. 3** Theoretical astronomical cycle solution. (a) The solution of La2010d. (b) MTM spectrum analysis. (c) Sliding window spectrum analysis.

peak in the spectrum is also obviously discontinuous at 2465 m and 2677.5 m (Fig. 4(c)). Because the logging sequence of some depths contains more noise, the high-frequency signal is suppressed by the noise with higher power (Crowley et al., 1992), which may also be due to the change in sedimentation rate caused by the change in depositional environment (Meyers et al., 2001).

The depth position of the discontinuous signal appears in the comprehensive consideration of the various characteristics of the GR logging sequence and slip spectrum (Fig. 4(d)). The whole target formation (2291−2900 m) was divided into three units, from bottom to top: unit 1 (2677.5−2900 m), unit 2 (2465−2677.5 m), and unit 3 (2291−2465 m), corresponding to Es4U, Es3L, and Es3M to Es3U strata. Then, the spectra of these three strata are analyzed (Figs. 4(e)−4(g)). The results showed that in unit 1 (2677.5−2900 m), the thickness periods corresponding to the five frequency spectrum peaks with higher than 95% confidence were 16.13 m, 8.7 m, 6.25 m, 3.88 m, and 3.11 m, with ratios of 96.9:52.26:

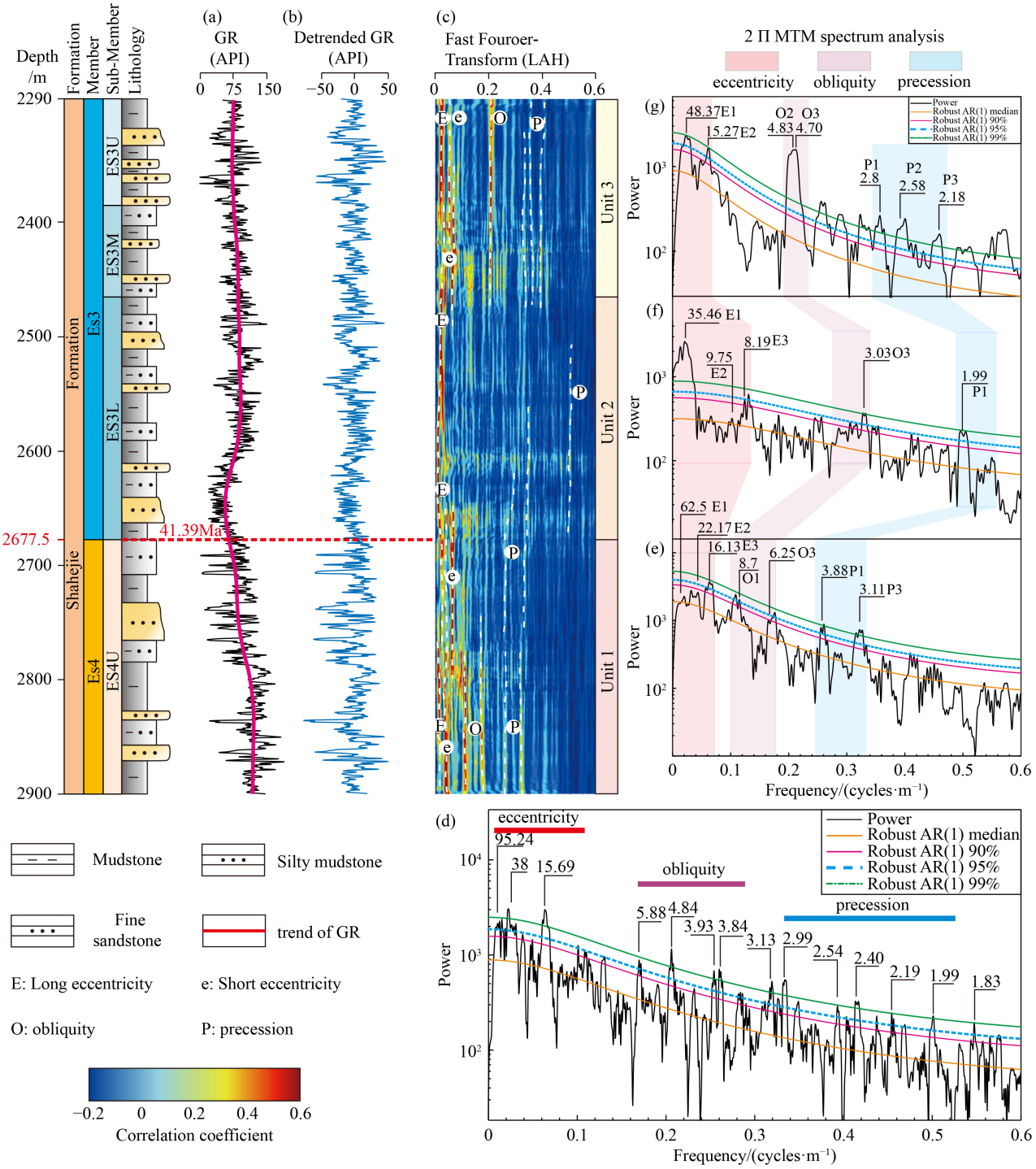


**Fig. 4** Cyclic stratigraphic analysis of C271 in the Chezhen Sag. (a) GR series from 2291 m to 2900 m (b) Detrended GR series. The red line is the long-term trends of the GR series. (c) Sliding window spectrum analysis of the GR series. (d) MTM spectrum analysis of the GR series. (e) MTM spectrum analysis of the Unit1 GR series from 2677.5 m to 2900 m. (f) MTM spectrum analysis of the Unit2 GR series from 2465 m to 2677.5 m. (g) MTM spectrum analysis of the Unit3 GR series from 2291 m to 2465 m.

37.54:23.3:18.68. These were the astronomical periods of E3, O1, O3, P1, and P3, respectively (Fig. 4(e)). In unit 2 (2465−2677.5 m), the thickness periods corresponding to the four frequency spectrum peaks with higher than 95% confidence were 35.46 m, 8.19 m, 3.03 m, and 1.99 m, with ratios of 405:93.6:36:22.72. These were the astronomical periods of E1, E3, O3, and P1, respectively (Fig. 4(f)). In unit 3 (2291−2465 m), the thickness periods corresponding to the seven frequency spectrum peaks with higher than 95% confidence were 48.37 m, 15.27 m, 4.83 m, 4.70 m, 2.8 m, 2.58 m, and 2.18 m, with ratios of 405:127.85:40.44:39.35:23.44:21.6:18.25. These are the

astronomical periods of E1, E2, O2, O3, P1, P2, and P3, respectively (Fig. 4(g)). The significant cycles identified by the three units from Es4U to Es3 were close to those identified by 405:125:96.9:51.7:40.1:38.7:23.2:22:18.7, which indicates that the stratigraphic sedimentary period of the studied section was affected by the Milankovich cycle. Based on the sedimentary thickness corresponding to the long eccentricity cycle (405 kyr), the sedimentation rate of each formation was estimated as follows: the sedimentation rate of Es4U was approximately 15.4 cm/kyr, the sedimentation rate of Es3L was approximately 8.76 cm/kyr, and the sedimentation rate of Es3M to Es3U was approximately 11.9 cm/kyr. The sedimentation rate from Es4U to Es3 in C271 shows a trend of decreasing at first and then increasing.

### 4.3 Estimation of the optimal sedimentation rate

Based on the astronomical cycle identification of the study section by the traditional "ratio method", the COCO and the eCOCO are further used to analyze and estimate the sedimentation rate of the three units of strata to improve the accuracy of cycle identification (Cleveland, 1979). This method calculates the correlation coefficient of the product moment between the power spectrum of the astronomical solution and the paleoclimate alternative sequence under a series of test sedimentation rates (Li et al., 2019). Using the autoregressive model (AR1), Monte Carlo simulation tests the correlation and null hypotheses of signals driven by non-astronomical orbits. The significance level of $H_0$ in the test indicates the probability that the null hypothesis in the stratigraphic record is mistakenly rejected (Ma et al., 2014). Therefore, the smaller $H_0$ is, the more reliable the analysis results. The higher the correlation coefficient $\rho$ is, the lower the significance level of $H_0$, and the corresponding sedimentation rate is the optimal sedimentation rate.

The sedimentation rate test interval selected by COCO analysis in this study was 0−50 cm/kyr, the Monte Carlo simulation was 2000 times, and the maximum frequency was 0.08 1/kyr. It was calculated that when the sedimentation rates of unit 1, unit 2, and unit 3 in C271 are 16−16.5 cm/kyr, 7.99−9.01 cm/kyr, and 12.15 cm/kyr, respectively, the significance level of $H_0$ (null hypotheses that are mistakenly rejected, non-astronomical orbit driving signal) is lower than 0.01 (Fig. 5), and more than five astronomical orbit parameters are involved in the calculation. Additionally, the correlation coefficient ρ corresponding to these sedimentary rates also reaches the maximum.

The eCOCO analysis of this study selected a sedimentation rate range of 0−30 cm/kyr, a sliding step of 2.125 m, and a sliding window of 152.25 m. A total of 2000 Monte Carlo simulations were carried out, and the results shown in Fig. 6 were obtained, in which red indicates the optimal sedimentation rate at a specific depth. According to the frequency spectrum analysis, the preliminary estimation of the average sedimentation rate at different depths by the ratio method (15.4 cm/kyr, 8.76 cm/kyr, and 11.9 cm/kyr) was consistent with the evaluation of the optimal sedimentation rate by the eCOCO (Fig. 6(a)), e$H_0$SL (Fig. 6(b)), and the Number of contributing astronomical parameters (Fig. 6(c)) methods. It is demonstrated again that the combination of power spectrum bands selected in this study meets the astronomical orbit driving conditions.

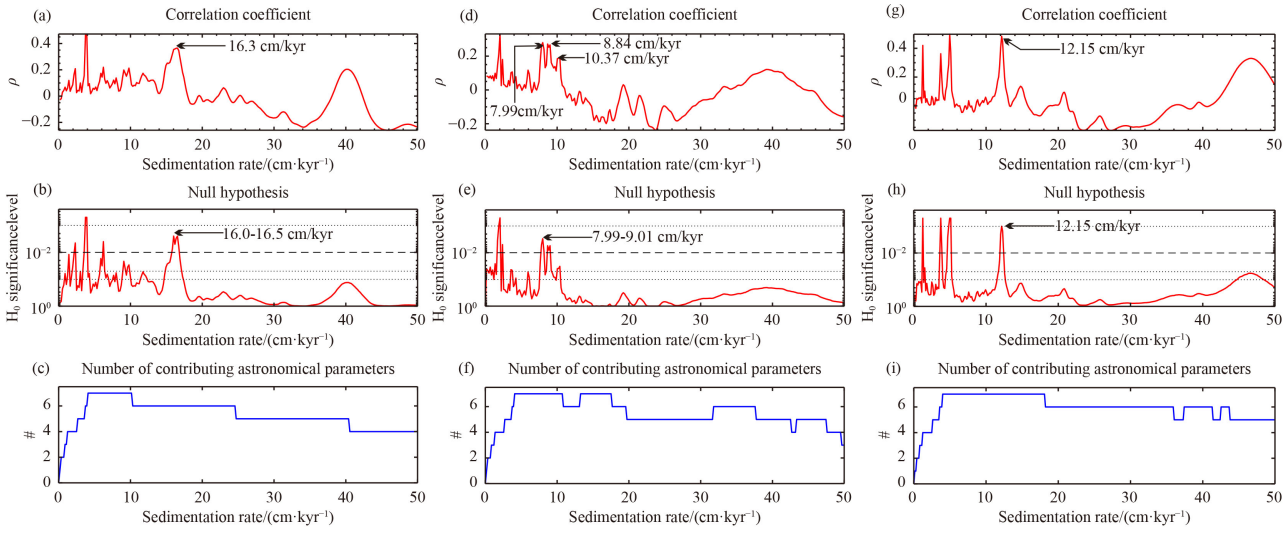


**Fig. 5** COCO analysis of C271 in the Chezhen Sag. (a−c) Correlation coefficient analysis, $H_0$ significance level analysis, and number of contributing astronomical parameters analysis of the Unit1 GR series, which from 2677.5 m to 2900 m. (d−f) Correlation coefficient analysis, $H_0$ significance level analysis, and number of contributing astronomical parameters analysis of the Unit2 GR series from 2465 m to 2677.5 m. (g−i) Correlation coefficient analysis, $H_0$ significance level analysis, and number of contributing astronomical parameters analysis of the Unit3 GR series, which from 2291 m to 2465 m.

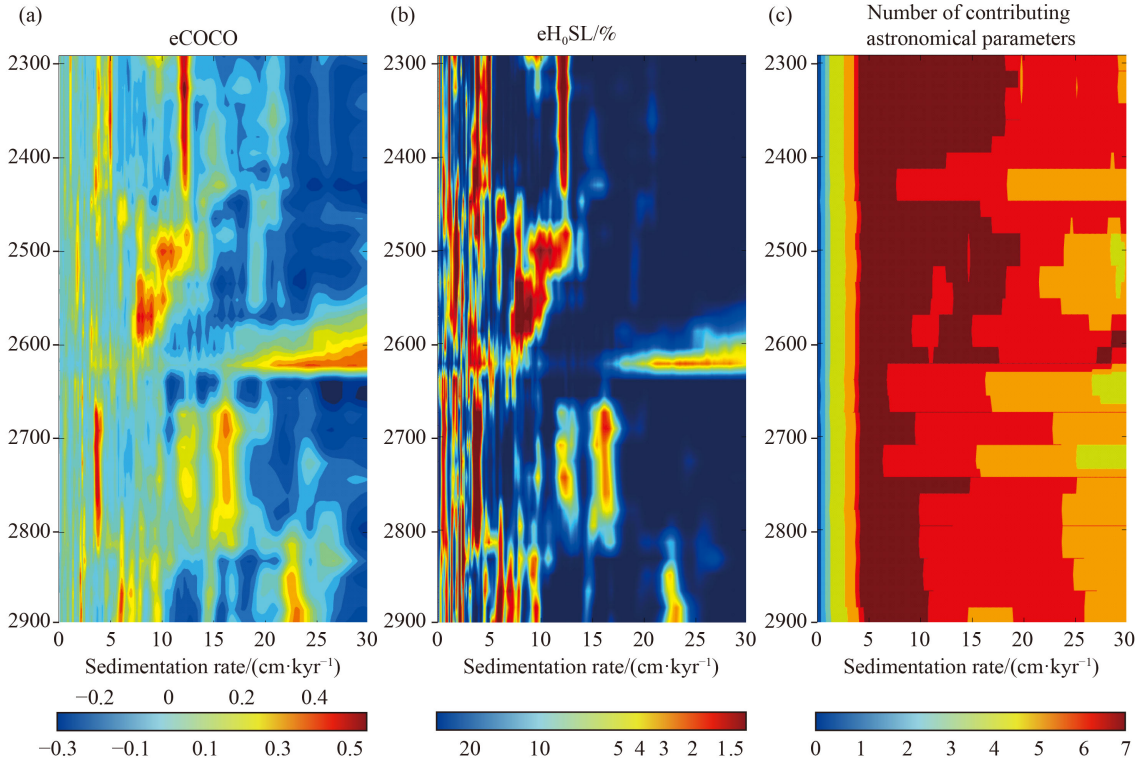


**Fig. 6** eCOCO analysis of C271 in Chezhen Sag. (a) eCOCO sedimentation rate of the GR series. (b) $eH_0SL$ sedimentation rate of the GR series. (c) Number of contributing astronomical parameters sedimentation rate of the GR series.

### 4.4 Time-depth conversion

Time-depth conversion is the key to establishing astronomical chronological scales in cyclic stratigraphy. Establishing high-precision and continuous astrogeological dating through time-depth conversion is a new method of geological dating. Earth's orbit is affected by the perihelion of Venus and Jupiter's orbits, resulting in a dominant high-amplitude 405 kyr eccentricity long period. Because Jupiter has a huge mass, it ensures the stability of the long period of 405 kyr eccentricity in the past hundreds of millions of years (Laskar et al., 2004). Based on Es3L and Es4U magnetic dating 41.39 Ma (Shi et al., 2019). The ages of the top and bottom of the GR filter curve at 405 kyr were 37.34 Ma and 42.87 Ma. Finally, the GR depth domain filter curve of 405 kyr (Fig. 7(b)) was tuned to the 405 kyr astronomical theory curve (Fig. 7(d)), the transformation of the filter curve from the depth domain to the time domain was realized (Fig. 7(f)), and the "floating" astronomical chronological scale from Es4U to Es3 in the Chezhen Sag was established (Fig. 7). Through the astronomical cycles identified above, it was found that there were 13.6 astronomical cycles with a long eccentricity of 405 kyr from Es4U to Es3 in the Chezhen Sag, which lasted for 5.53 Myr. The GR filtering curve of 40.1 kyr (Fig. 7(c)) was also tuned to the 405 kyr astronomical theory curve, and an astronomical chronological scale with a resolution of 40.1 kyr was obtained (Fig. 7(g)). Further calculation showed that there were 37 astronomical cycles with an obliquity of 40.1 kyr in Es4U, which lasted for 1.48 Myr. There were 66 astronomical cycles with an obliquity of 40.1 kyr in Es3L, which lasted for 2.66 Myr. There were 35 astronomical cycles with an obliquity of 40.1 kyr from Es3M to Es3U, which lasted for 1.39 Myr. According to the tuned 40.1 kyr cycle curve, the sedimentary rate change from Es4U to Es3 was calculated (Fig. 7).

### 4.5 Sedimentary noise indicative of paleolake levels

Based on the sedimentary noise model $\rho 1$, the sedimentary noise model of the GR depth sequence (Fig. 8(a)) was assumed and calculated, and the relative lake level variation curve (Fig. 8(b)) during the sedimentary period from Es4U to Es3 was obtained. By reconstructing the sedimentary noise curve of the GR time series (Fig. 8(d)), two curves, $\rho 1$ (Fig. 8(g)) and DYNOT (Fig. 8(h)), which can replace the relative sea level change in the same sedimentary period, were obtained. The $\rho 1$ and DYNOT curves of well C271 from the Es4U to Es3 deposition periods show similar simulation results. During the whole deposition period, there were five significantly enhanced noises (gray shading), all of which appeared in the low-value area of the eCOCO spectrum correlation coefficient (Fig. 8(c)), relatively shallow water, and an unstable depositional environment.

After filtering the GR data in the time domain, the

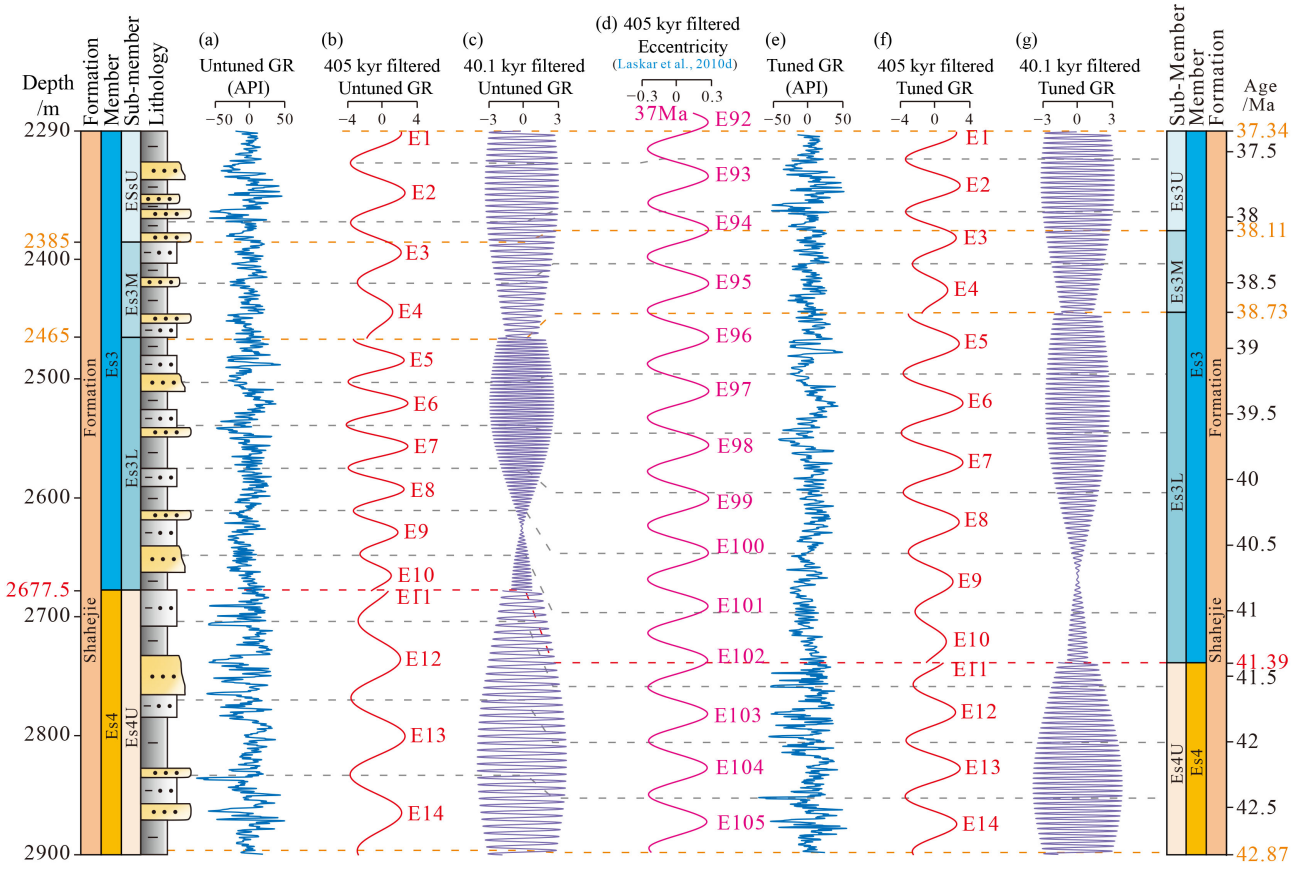


**Fig. 7** Astronomical time scale (ATS) for the middle Eocene succession of C271 in the Chezhen Sag. (a) Untuned GR series of C271 (2291–2900 m). (b) 405 kyr filtered Untuned GR series in the depth domain. (c) 40.1 kyr filtered Untuned GR series in the depth domain. (d) 405 kyr filtered eccentricity curve of the La2010 solution. (e) Tuned GR series of C271 (37.34–42.87 Ma). (f) 405 kyr filtered tuned GR series in the time domain. (g) 40.1 kyr filtered tuned GR series in the time domain.

astronomical cycle curve of 1.2 Myr ultra-long obliquity was obtained and compared with the relative lake level change curve of the Miocene in the Chezhen Sag simulated by the $\rho 1$ and DYNOT sedimentary noise models. The results showed that the relative lake level change corresponds to the inverse phase of the 1.2 Myr ultra-long obliquity astronomical cycle curve, that is, the maximum corresponding ultra-long obliquity in shallow water close to the lake level. We believe that during the Middle Eocene in Chezhen Sag, the relative lake level change was regulated by astronomical orbit and divided into four sequences (Fig. 8(h)) according to the maximum lake level change.

## 5 Discussion

### 5.1 Astronomical time scales of the Jiyang Depression

Predecessors have carried out many practical works in the Jiyang Depression of the Bohai Bay Basin. Liu et al. (2018) used the GR logging data of the Shengke-1 well in the Dongying Sag as an alternative index, taking the Paleogene and Neogene boundary age of 23.03 Ma at the top of the Dongying Formation as the "anchor point" (Gradstein et al., 2012), established an astronomical chronological scale, and calculated that the absolute age of the boundary between Es3 and Es4 was 42.47 Ma, the top age of Es3 was 35.99 Ma, and all of Es3 persisted at 6.48 Myr (Fig. 9). The "floating" astronomical year established in this paper represents the top age of Es3 as 37.34 Ma, which is within the range of the Es3 astronomical chronological scale based on Liu et al. (2018). Zhang and Jin (2021) used the GR logging data of the Luo-69 well in the Zhanhua Sag as an alternative index and used volcanic ash dating 42.47 Ma at the boundary between Es3L and Es4U as the "anchor point" (Liu et al., 2018) to establish an astronomical chronological scale, in which the top boundary age of Es3L is 40.128 Ma, and the whole Es3L lasted for 2.342 Myr (Fig. 9). The Es3L astronomical year representative established in this study was younger than the Es3L "floating" astronomical year representative based on Zhang and Jin (2021), but the sedimentary rate and duration are almost the same. The main difference is that the "anchor point" they use is volcanic ash dating, which is 1 Myr older than our magnetic dating. Shi et al. (2019) used the MS data of the Fanye-1 well in the Dongying

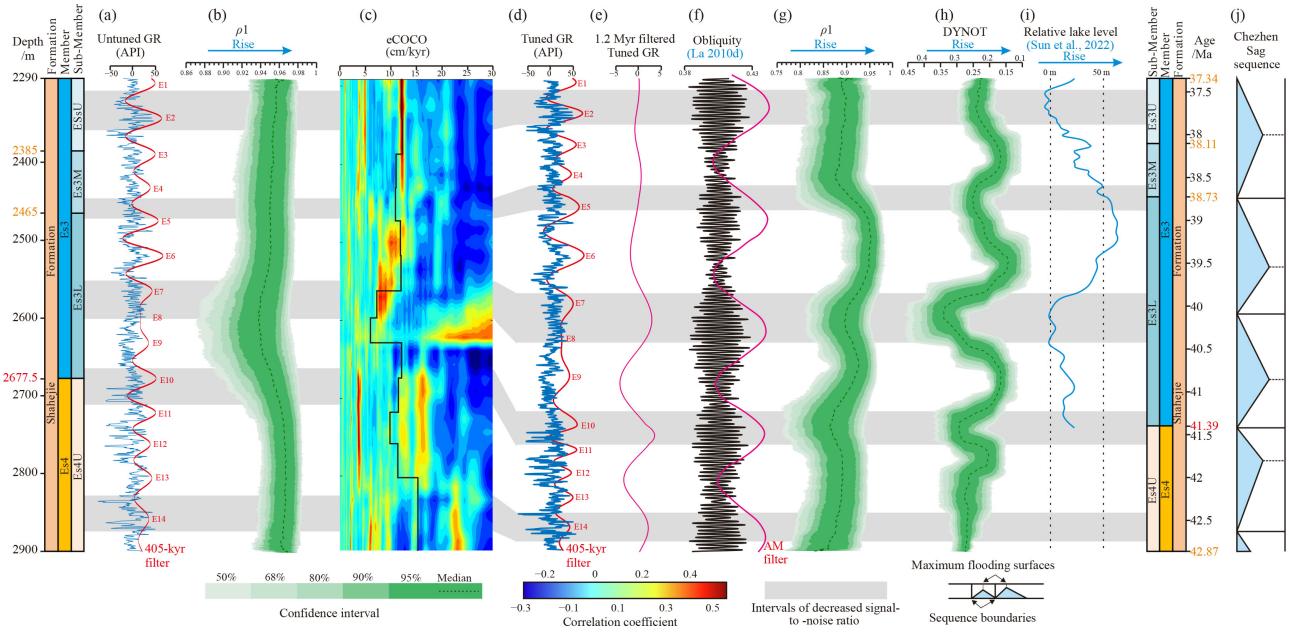


**Fig. 8** Sedimentary noise model interpretation of lake-level variations in C271. (a) Untuned GR series (blue) of C271(2291–2900 m) with 405 kyr filtered output (red). (b) $\rho$1 model of Untuned GR series. (c) eCOCO analysis (from Fig. 6) with the sedimentary rate (black). (d) Tuned GR series (blue) of C271 (37.34–42.87 Ma) with 405 kyr filtered output (red). (e) 1.2 Myr filtered tuned GR series. (f) Earth's obliquity solution (black, Laskar et al., 2011) and its 1.2 Myr-AM cycles (red). (g, h) $\rho$1 and DYNOT models of the tuned GR series. (i) Lake level fluctuations of the 3rd Member of Paleogene Shahejie Formation, Chezhen Sag, Bohai Bay Basin (Sun et al., 2022). (j) Chezhen Sag sequences from lake level change.

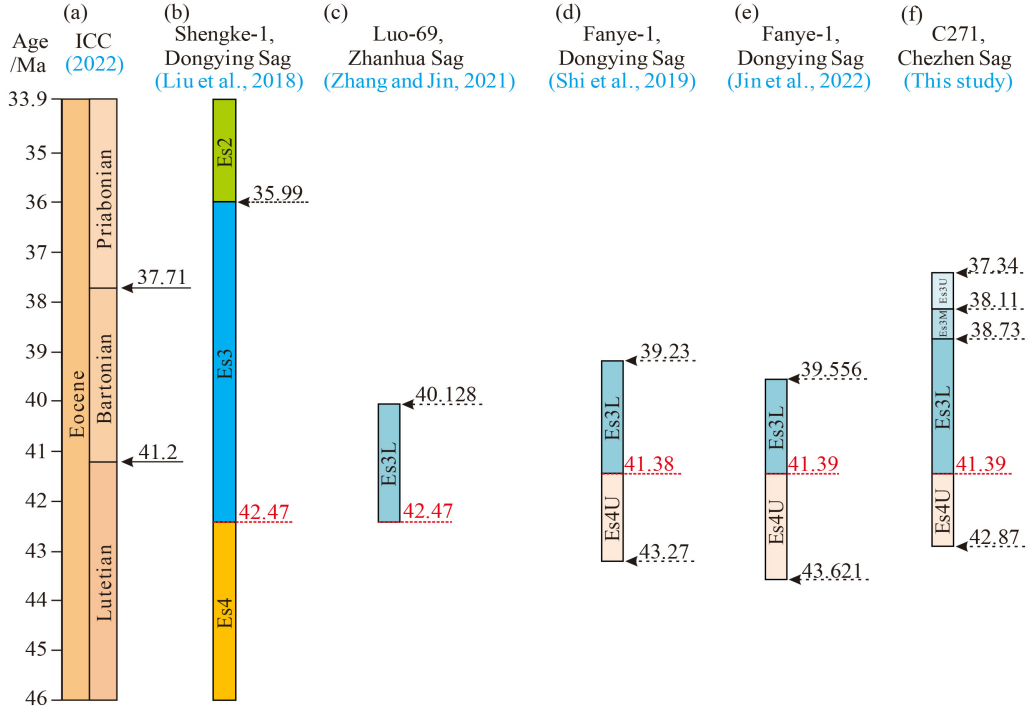


**Fig. 9** Astronomical time scales (ATS) of the Jiyang Depression. (a) ICC, International Chronostratigraphic Chart, 2022. (b) ATS of Dongying Sag was established by well Shengke-1 (Liu et al., 2018). (c) ATS of Zhanhua Sag was established by well Luo-69 (Liu et al., 2018). (d, e) ATS of Dongying Sag was established by well Fanye-1 (Shi et al., 2019; Jin et al., 2022). (f) ATS of Chezhen Sag was established by well Che-271 (This study).

Sag as a substitute index and took the magnetic dating age 41.39 Ma at the boundary between Es3L and Es4U as the "anchor point" to establish an astronomical chronological scale in which the top age of Es3L was 39.23 Ma, the bottom age of the whole Es3L lasting 2.16 Myr, Es4U is 43.27 Ma, and the entire Es4U lasted 1.88

Myr (Fig. 9). Jin et al. (2022) used the GR logging data of the Fanye-1 well in the Dongying Sag as an alternative index, and took the magnetic dating age 41.39 Ma at the boundary between Es3L and Es4U as the "anchor point" (Shi et al., 2019) to establish an astronomical chronological scale, in which the top age of Es3L was 39.556 Ma, the bottom age of the whole Es3L lasted 1.83 Myr, Es4U was 43.621 Ma, and the entire Es4U lasted 2.231 Myr (Fig. 9). In this study, the bottom of Es4U in well C271 was not drilled, so it is younger than the bottom age of Es4U of Shi et al. (2019) and Jin et al. (2022). We found that the deposition of the Middle Eocene in the Jiyang Depression of the Bohai Bay Basin was regulated by the astronomical cycle, and the study of cyclic stratigraphy in different sags was slightly different. Nevertheless, the overall sedimentation rate and duration were almost the same. The reasons for the differences in the representation of astronomical years mainly include two points: one is the different selection of "anchor points" for the establishment of "floating" astronomical time scales, and the other is the influence of the geographical location of the region. The "floating" astronomical time scale established in the text is credible.

## 5.2 Astronomically forced paleolake level variations

The Earth's orbital parameters affect the climate and change the depositional environment (Rachold and Brumsack, 2001). The change in eccentricity indicates the evolution in the orbital plane of the Earth around the Sun and then affects the change in insolation. With the increase in eccentricity, the Earth's orbit around the sun changes from near-circle to ellipse, the eccentricity decreases, and the Earth's orbit around the sun changes from ellipse to near-circle, but the direct effect of the eccentricity period on sunlight is less than 1% (Berger, 1988; Huang, 2014). At present, the rotation axis of the earth is inclined by about 23.26 from the "vertical" direction. The inclination of the earth's rotation axis fluctuates in the range of 22.5° to 24.5° (Hinnov, 2013; Huang, 2014). The greater the inclination of the earth's axis, the more extreme our seasonal differences will be. Because each hemisphere receives more solar radiation in summer (the hemisphere tilted to the sun side is summer). A large tilt angle is beneficial to the melting and recession of glaciers (Steven, 2021).

Sun et al. (2022) used a variety of geochemical indicators and methods concluding Adams' formula and Couch's method were adopted to reveal the paleosalinity and lake level variations of the Es3 of Chezhen Sag (Fig. 8(i)). Comparing it with the relative lake level change of the same period based on sedimentary noise models (DYNOT). We found that there was a similar change trend between them, and the lake level reached the lowest during 40.5−40 Ma (Fig. 8). This study, 1.2 Myr ultra-long obliquity is in the maximum period, corresponding to the maximum of obliquity amplitude modulation period (Laskar et al., 2011), at the same time corresponding to the relatively shallow water depositional environment while corresponding to the sequence boundary. 1.2 Myr ultra-long obliquity is in the minimum period, corresponding to the minimum of obliquity amplitude modulation period (Laskar et al., 2011), at the same time corresponding to a fairly deep water depositional environment, and the maximum lake flooding surface (Fig. 8). Our explanation for this is that during the maximum period of 1.2 Myr, the obliquity of the earth's axis is at a high value for a long time, the meridional sunshine of the earth increases, the evaporation of the lake increases, and the seasonal contrast is large, and finally the lake level drops (Fig. 10(a)). During the minimum period of 1.2 Myr, the obliquity of

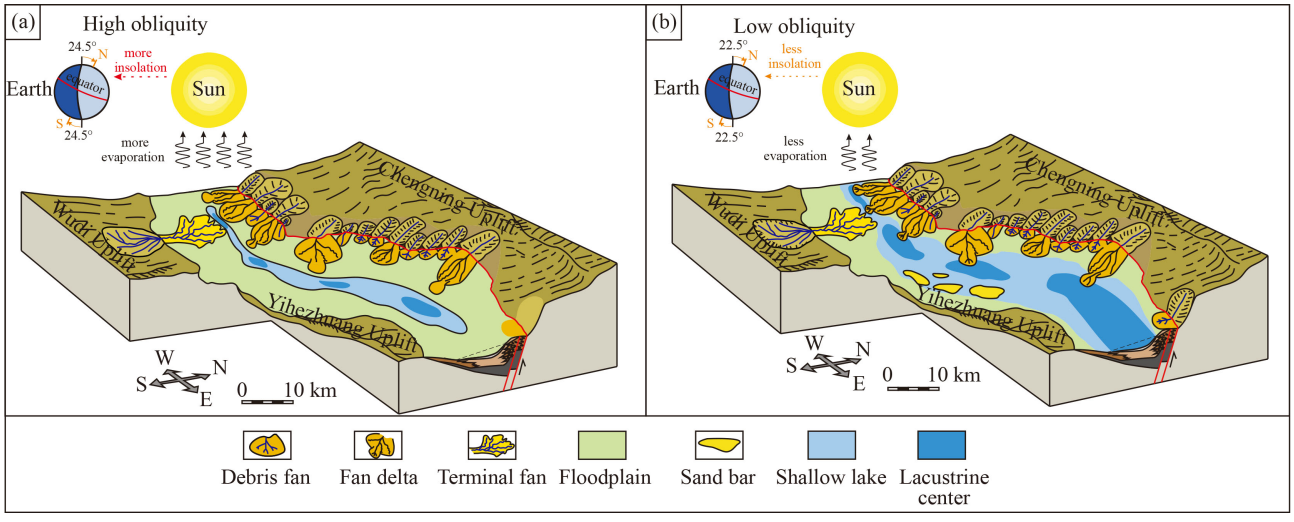


**Fig. 10** Astronomically forced paleolake level variations in the Middle Eocene Chezhen Sag. (a) High obliquity forced paleolake level variations. (b) Low obliquity forced paleolake level variations.

the earth's axis is at a low value for a long time, the meridional sunshine of the earth is weakened, the evaporation of the lake is less, and the seasonal contrast is small, and finally the lake level rises (Fig. 10(b)).

## 6 Conclusions

1) Based on the time series analysis, the astronomical chronological scale of the Middle Eocene in the Chezhen Sag with a resolution of 40.1 kyr is established. The number of "40.1 kyr" obliquity cycles from Es4U to Es3 in the Chezhen Sag were 138, covering a duration of 5.53 Myr. Among them, the number of "40.1 kyr" obliquity cycles in Es4U were 37, lasting 1.48 Myr. The number of "40.1 kyr" obliquity cycles in Es3L were 66, lasting 2.66 Myr. The number of "40.1 kyr" obliquity cycles from Es3M to Es3U were 35, lasting 1.39 Myr.

2) Through COCO analysis and eCOCO analysis, it is found that the optimal sedimentary rate of Es4U was 15.4 cm/kyr, the optimal sedimentary rate of Es3L was 8.76 cm/kyr, and the optimal sedimentary rate from Es3M to Es3U was 11.9 cm/kyr.

3) The sedimentary noise simulation reveals the history of the change in paleolake water in the Middle Eocene in the Chezhen Sag, according to which four sequences are divided. In particular, there is a good correlation between the filtered 1.2 Myr period and the relative lake level change, and the inverse phase corresponds. This may be an essential driving factor for the evolution of the water surface of the ancient lake in the Chezhen Sag.

## References


Aplin A C, Macquaker J S H (2011). Mudstone diversity: origin and implications for source, seal, and reservoir properties in petroleum systems. AAPG Bull, 95(12): 2031–2059

Berger A (1988). Milankovitch theory and climate. Rev Geophys, 26(4): 624–657

Chen T, Zhang J L, Li Y, Zhao Y F (2021). Quantitative reconstruction of the palaeoclimate of the Shahejie Formation in the Chezhen Depression, Bohai Bay Basin, eastern China. Front Earth Sci, 15(4): 909–921

Chen X Y, Xu Y G, Menzies M (2014). Tephrochronology: principles and applications. Acta Petrol Sin 30(12): 3491–3500 (in Chinese)

Cleveland W S (1979). Robust locally weighted regression and smoothing scatterplots. J Am Stat Assoc, 74(368): 829–836

Crowley T J, Kim K Y, Mengel J G, Short D A (1992). Modeling 100, 000-year climate fluctuations in pre-pleistocene time series. Science, 255(5045): 705–707

Feng Y L, Jiang S, Hu S Y, Li S T, Lin C S, Xie X N (2016). Sequence stratigraphy and importance of syndepositional structural slope-break for architecture of Paleogene syn-rift lacustrine strata, Bohai Bay Basin, E. China. Mar Pet Geol, 69: 183–204

Freytet P, Verrecchia E P (2002). Lacustrine and palustrine carbonate petrography: an overvie. J Paleolimnol, 27(2): 221–237

Gradstein F, Ogg J G, Schmitz M D, Ogg G M (2012). The Geologic Time Scale (2 vols). Amsterdam: Elsevier

Hao F, Zhou X H, Zhu Y M, Yang Y Y (2009). Mechanisms for oil depletion and enrichment on the Shijiutuo uplift, Bohai Bay Basin, China. AAPG Bull, 93(8): 1015–1037

Hays J D, Imbrie J, Shackleton N J (1976). Variations in the earth's orbit: pacemaker of the ice ages. Science, 194(4270): 1121–1132

Hinnov L A (2013). Cyclostratigraphy and its revolutionizing applications in the earth and planetary sciences. Geol Soc Am Bull, 125(11–12): 1703–1734

Hinnov L A, Hilgen F J (2012). Cyclostratigraphy and astrochronology. In: Gradstein F M, Ogg J G, Schmitz M D, eds. The Geologic Time Scale. Amsterdam: Elsevier, 63–83

Huang C J (2014). The current status of cyclostratigraphy and astrochronology in the Mesozoic. Earth Sci Front, 21(2): 48–66

Huang C J, Hinnov L A (2019). Astronomically forced climate evolution in a saline lake record of the middle Eocene to Oligocene, Jianghan Basin, China. Earth Planet Sci Lett, 528: 115846

Jin S D, Deng H C, Zhu X, Liu Y, Liu S B, Fu M Y (2020). Orbital control on cyclical organic matter accumulation in Early Silurian Longmaxi Formation shales. Geosci Front, 11(2): 533

Jin S D, Liu S B, Li Z, Chen A Q, Ma C (2022). Astrochronology of a middle Eocene lacustrine sequence and sedimentary noise modeling of lake-level changes in Dongying Depression, Bohai Bay Basin. Palaeogeogr Palaeoclimatol Palaeoecol, 585: 110740

Laskar J, Fienga A, Gastineau M, Manche H (2011). La2010: a new orbital solution for the long-term motion of the Earth. Astron Astrophys, 532: A89

Laskar J, Robutel P, Joutel F, Gastineau M, Correia A C M, Levrard B (2004). A long-term numerical solution for the insolation quantities of the Earth. Astron Astrophys, 428(1): 261–285

Li G S, Wang Y B, Lu Z S, Liao W, Song G Q, Wang X J, Xu X Y (2014). Geobiological processes of the formation of lacustrine source rock in Paleogene. Sci China Earth Sci, 57(5): 976–987

Li M S, Hinnov L A, Kump L (2019). Acycle: time-series analysis software for paleoclimate research and education. Comput Geosci, 127: 12–22

Li M S, Ogg J, Zhang Y, Huang C J, Hinnov L A, Chen Z Q, Zou Z Y (2016). Astronomical tuning of the end-Permian extinction and the Early Triassic Epoch of South China and Germany. Earth Planet Sci Lett, 441: 10–25

Li M, Hinnov L A, Huang C, Ogg J G (2018). Sedimentary noise and sea levels linked to land-ocean water exchange and obliquity forcing. Nat Commun, 9(1): 1004

Liu Z H, Huang C J, Algeo T J, Liu H M, Hao Y Q, Du X B, Lu Y C, Chen P, Guo L Y, Peng L (2018). High-resolution astrochronological record for the Paleocene-Oligocene (66–23 Ma) from the rapidly subsiding Bohai Bay Basin, northeastern China. Palaeogeogr Palaeoclimatol Palaeoecol, 510: 78–92

Luan X W, Kong X X, Zhang J L, Jiang L, Peng Y X, Cai Y (2022). Astronomical forcing of origins of Eocene carbonate-bearing fine-grained sedimentary rock in Dongying Sag. Acta Sediment Sin, 42(2): 688–700 (in Chinese)

Ma C, Meyers S R, Sageman B B, Singer B S, Jicha B R (2014).

Testing the astronomical time scale for Oceanic Anoxic Event 2, and its extension into Cenomanian strata of the Western Interior Basin (USA). Geol Soc Am Bull, 126(7–8): 974–989

Meyers S R, Sageman B B, Hinnov L A (2001). Integrated quantitative stratigraphy of the Cenomanian-Turonian bridge creek limestone member using evolutive harmonic analysis and stratigraphic modeling. J Sediment Res, 71(4): 628–644

Rachold V, Brumsack H J (2001). Inorganic geochemistry of Albian sediments from the Lower Saxony Basin NW Germany: palaeoenvironmental constraints and orbital cycles. Palaeogeogr Palaeoclimatol Palaeoecol, 174(1/2/3): 121–143

Shi J Y, Jin Z J, Liu Q Y, Zhang R, Huang Z K (2019). Cyclostratigraphy and astronomical tuning of the middle eocene terrestrial successions in the Bohai Bay Basin, Eastern China. Global Planet Change, 174: 115–126

Steven E (2021). Earth’s orbital variations. In: Steven E, ed. A Brief History of the Earth’s Climate, 63–75

Su J B, Zhu W B, Wei J, Xu L M, Yang Y F, Wang Z Q, Zhang Z Y (2011). Fault growth and linkage: implications for tectonosedimentary evolution in the Chezhen Basin of Bohai Bay, eastern China. AAPG Bull, 95(1): 1–26

Sun L, Zhang J L, Li Y, Yan X, Zhang X C (2022). Paleosalinity and lake level fluctuations of the 3rd Member of Paleogene Shahejie Formation, Chezhen Sag, Bohai Bay Basin. Front Earth Sci, 16(4): 949–962

Thomson D J (1982). Spectrum estimation and harmonic analysis. Proc IEEE, 70(9): 1055–1096

van Vugt N, Langereis C G, Hilgen F J (2001). Orbital forcing in Pliocene–Pleistocene Mediterranean lacustrine deposits: dominant expression of eccentricity versus precession. Palaeogeogr Palaeoclimatol Palaeoecol, 172(3/4): 193–205

Wang M (2020). Astronomical forcing and sedimentary noise modeling of lake-level changes: case studies from the late Triassic Newark Basin, USA and Paleogene Eastern China Basins. Dissertation for Doctoral Degree. Beijing: China University of Geosciences

Wang M, Chen H H, Huang C J, Kemp D B, Xu T W, Zhang H G, Li M S (2020). Astronomical forcing and sedimentary noise modeling of lake-level changes in the Paleogene Dongpu Depression of North China. Earth Planet Sci Lett, 535: 116116

Wang S Y (2017). Seismic-geological comprehensive research on the effectiveness of compact glutenite reservoirs in the west of Chezhen Sag. Dissertation for Doctoral Degree. Qingdao: China University of Petroleum (East China) (in Chinese)

Wang Y Z, Cao Y C (2010). Lower property limit and controls on deep effective clastic reservoirs of Paleogene in Chezhen Depression. Acta Sediment Sin, 28(04): 752–761

Wu H C, Zhang S H, Hinnov L A, Jiang G Q, Yang T S, Li H Y, Wan X Q, Wang C S (2014). Cyclostratigraphy and orbital tuning of the terrestrial upper Santonian–Lower Danian in Songliao Basin, northeastern China. Earth Planet Sci Lett, 407: 82–95

Yao X, Zhou Y Q, Hinnov L A (2015). Astronomical forcing of a Middle Permian chert sequence in Chaohu, south China. Earth Planet Sci Lett, 422: 206–221

Yao Y M, Liang H D, Cai Z G (1994). Tertiary in Petroliferous Regions of China: IV, the Bohai Bay Basin. Beijing: Petroleum Industry Press (in Chinese)

Zhang R L, Jin S D (2021). Cyclostratigraphy research on lower Member 3 of Shahejie Formation in Well Luo 69 in Zhanhua Sag Bohai Bay Basin. J Cent South Univ (Sci and Technol), 52(5): 1516–1531

Zhang Z F, Huang Y J, Li M S, Li X, Ju P C, Wang C S (2022). Obliquity-forced aquifer-eustasy during the Late Cretaceous greenhouse world. Earth Planet Sci Lett, 596: 117800

Zhou Y, Jin S D, Liu Y, Liu S B, Zhang Q L (2024). Cyclostratigraphy research on well-logging of the Lower Cambrian Qiongzhusi Formation in southwestern Sichuan Basin. Acta Sediment Sin, 42(01): 142–157